Noname manuscript No.
(will be inserted by the editor)

Analysis of time variable GRACE temporal models

Greenland ice mass loss

Shivam Pandey(17807671) · Sarvesh Chaudhary(170637)

Received: date / Accepted: date

Abstract The Gravity Field and Steady-State Ocean Circulation Explorer (GOCE) launched by ESA's Living Planet Program satellites has improved the spatial resolution of the gravity measurements. Before this the GRACE was there in the use with higher temporal resolution. The field of ocean circulation is crucial in the environmental studies, thus we need to analyse the currents in the ocean at local level, but due to not enough spatial resolution of the GRACE mission the estimated currents were degraded in the precision. Later with the used use of GOCE the enough spatial resolution of the geoid was achieved and could be used in the ocean circulation estimation. The work contains our study on the ocean circulation from the altimetry and the GOCE data. The work presents the ocean circulation estimation in the region of Bay of Bengal. We will also propose the analysis method for the ocean currents in order to get more information from the estimates.

Keywords GOCE · Altimetry · Ocena currents · JASON2 · SARAL · Clustering

1 Introduction

The Gravity Field and Steady-State Ocean Circulation Explorer (GOCE) launched by ESA's Living Planet Program in 17th MARCH 2009, was a huge boost to the geoid estimation with more spatial resolutio. Before this the GRACE mission was used in the Earth's gravity measurements was meant to have more temporal resolution. The GRACE mission has provided a lot of precious information like ice mass changes etc. But the problem when it comes to an application where we need spatial preciseness and accuracy, the GRACE is unable to provide such kind of spatial resolution, and here comes the GOCE mission launched in year2009. The GOCE mission provides gravity readings with higher spatial resolution. The problem of the ocean currents monitoring is that it needs to be spatially more precise unless would be prone to noise. The data of GOCE was suitable for the ocean circulation monitoring. In this work we will show the ocean current currents extraction and the analysis. We have used satellite altimetry to get the sea surface height and then getting the gradients w.r.t latitude and longitude.

2 Ocean Topography

The ocean circulation can be determined by observing the changes of ocean surface relative to some stationary surface. Figure 1 by [HercegHerceg] provides the complete illustration on the dynamic ocean topography.

Address(es) of author(s) should be given

2.1 Geoid & Inst. Sea Surface Height

For this purpose if fixed surface geoid is chosen. The measurement of geoid comes from the GOCE [Becker, Brockmann SchuhBecker .2014] [Bingham, Knudsen, Andersen PailBingham .2011] as we have also mentioned it previously that the GRACE is more temporally sound, while the GOCE is more spatially sound, so we have used a static model of geoid computed from both the GRACE and GOCE data. The sea surface height is provided by the altimetry data $h(t)$ [Bingham, Haines LeaBingham .2015]. The altimetry helps in obtaining the instantaneous sea height over the ellipsoidal surface. the groid model also provide the height of geoid N over the sea surface.

2.2 Inst. Dynamic Ocean Topography

The instantaneous dynamic ocean topography can be calculated as the instantaneous sea height variation over the static surface and in our case the static surface is taken as geoid. The instantaneous dynamic ocean topography $\eta(t)$ is given by equation: [ChristianChristian2012]

$$\eta(t) = h(t) - N \tag{1}$$

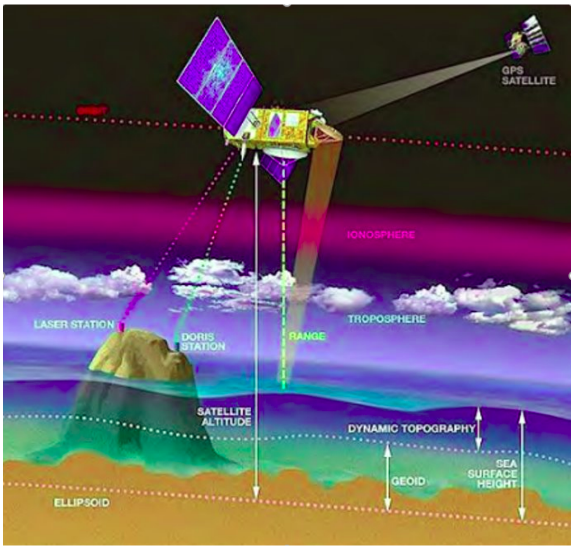

Fig. 1: Working of satellite altimetry and geoid in dynamic ocean topography.

The instantaneous dynamic ocean topography $\eta(t)$ is affected by local and sudden disruptions from atmosphere or artificial sources, so in order to get the consistent variation of the dynamic ocean we need to work on the assumption of constant path for satellite altimetry that means we can go for an average for the same trajectory over a long period of time in order to get rid of these sudden disruptions in the sea [van der Meijde, Pail, Bingham Floberghagenvan der Meijde .2015]. Mean dynamic ocean topography $\overline{\eta}$ can be found out by equation [**?**]:

$$\overline{\eta} = \frac{\sum_t h(t)}{N} - N \tag{2}$$

The above equation shows the information about a single satellites constant trajectory assumption, we need to do it for all the satellite trajectories. Figure 2 shows the example of obtained mdt from ssh geoid pipeline.

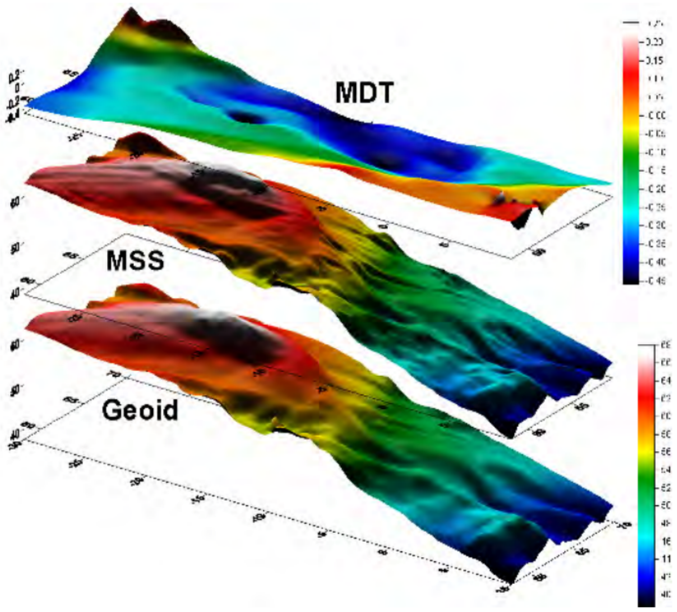

Fig. 2: SSH, Geoid, and obtained MDT example

3 Data Acquisition

Here we would need 2 main dataset one is the geoid calculated for the area of interest and the other is the satellite altimetry dataset for approximately same region. We have acquired the geoid datasete from the ICGEN website, here we have used the $ICGT\_R1C$ model for calculation of the geoid as it contains both the GRACE and GOCE data.

For the altimetry data we have used the OpenADB dataset. The dataset is already been converted to WGS84 reference system is provided here, and we are going to use the dataset of JASON2 and SARAL satellites for our experements in the region of interest and that is Bay of Bengal. Figure 3 shows the geoid data acquisition process from GOCE and GRACE and Figure 4 shows the ssh data acquisition process from JASON2 and SARAL [ChristianChristian2012].

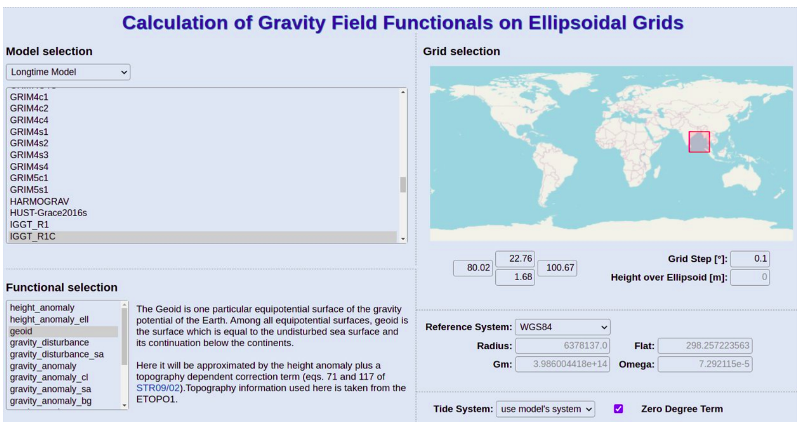

Fig. 3: Geoid data acquisition.

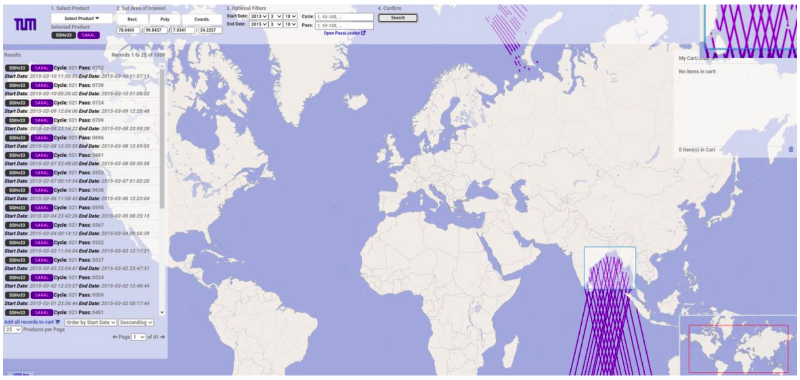

Fig. 4: SSH data acquisition.

4 Filtering

In order to account for the noise in the signal, particularly for coefficients of high degree, it is necessary to filter the data set obtained from the GOCE and the SSH datas. Here the effect of interpolation of the satellite altimetry data in the region of interest provides the inconsistencies in the area therefore we will be using the Gaussian filter as a remedy to this. Other authors have also provided the information about the other kind of specialised filters. In order to keep things simple we will be using a $1.2°x1.2°$ filter size to get rid of unwanted noise [Bingham, Knudsen, Andersen PailBingham .2011] [Bingham, Haines LeaBingham .2015].

5 Ocean currents

Once we have filtered the mean dynamic topography (mdt) $\overline{\eta}$ the ocean circulation can be computed from the method of differentiation in the spherical domain. Equation 3 shows the procedure to obtain the current components at a certain lat long. [Haines .Haines .2011] [Rio, Mulet PicotRio .2014] [Becker, Brockmann SchuhBecker .2014] [Knudsen, Bingham, Andersen RioKnudsen .2011] [Baltazar Andersen .Baltazar Andersen .2018] [Janjić .Janjić .2012] [Haines .Haines .2011] [Vigo, Sempere, Chao TrottiniVigo .2018] [Pail .Pail .2010].

$$
\begin{aligned}
&u = -\frac{\gamma}{fR}\frac{\partial\overline{\eta}}{\partial\phi} \\
&v = -\frac{\gamma}{fR\cos\phi}\frac{\partial\overline{\eta}}{\partial\lambda} \\
&\text{Where} \\
&f = 2\omega_e\sin\phi
\end{aligned}
\tag{3}
$$

6 Results

The complete process of the current component estimation is provided in the flow-chart 5. Let's follow the step to get the final current component and analyse that.

6.1 Geoid calculation

We have acquired a geoid grid of $0.1°x0.1°$ resolution from the ICGEM website and shown in the Figure 6 shows the geoid height N from the $WGS84$ ellipsoid.

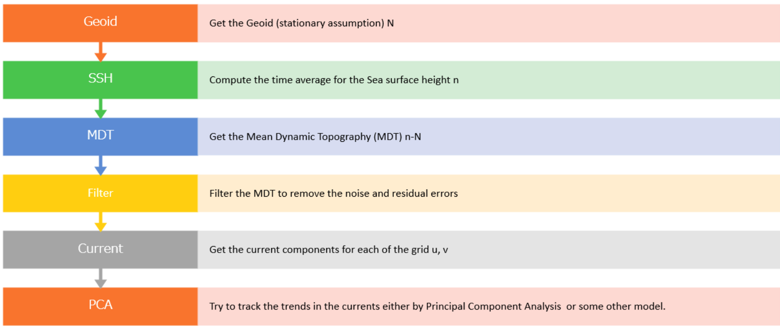

Fig. 5: Flow chart for the data processing and analysis.

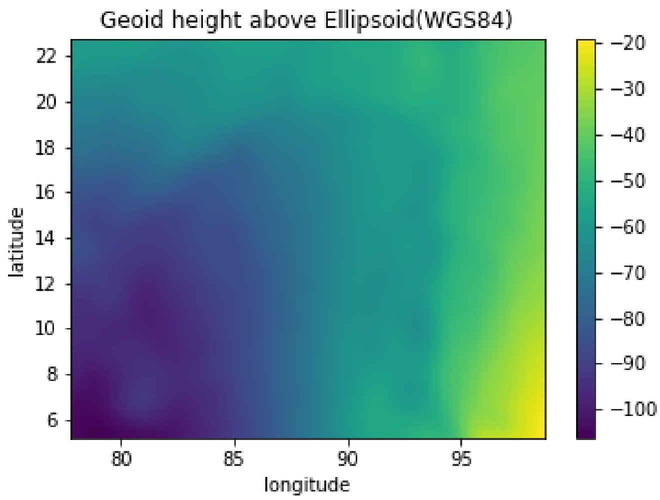

Fig. 6: Geoid grid IO result.

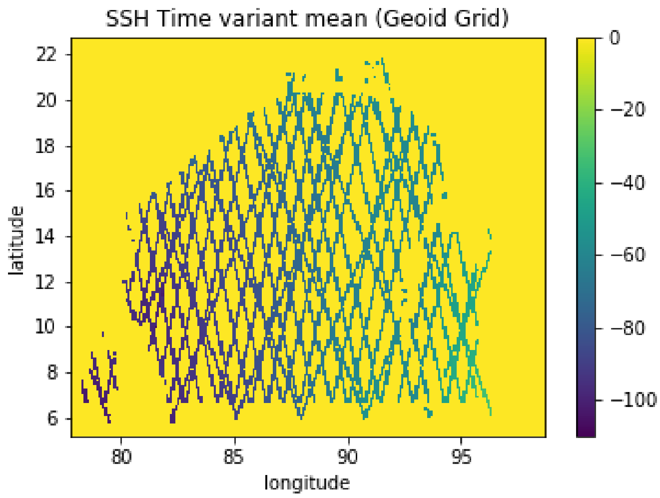

Fig. 7: Sea Surface Height data.

6.2 SSH data acquisition and Interpolation

We have got the Sea surface height data from the OpenADB website for the ROI associated with satellite missions JASON2 ans SARAL. Figure 7 shows the temporal mean of the SSH data adjusted to the geoid grid on resolution of $0.1° X 0.1°$. As we can see here, lot of data is missing in order to fill that data we have interpolated the complete data. Figure 8 shows the interpolated SSH data contained in the convex-hull of the system.

Note: *We have used here the convex-hull instead of coastal boundary as that is computational entity defining the enclosing boundary of data. This has been imposed as to overcome the lack of coastal region boundary data.*

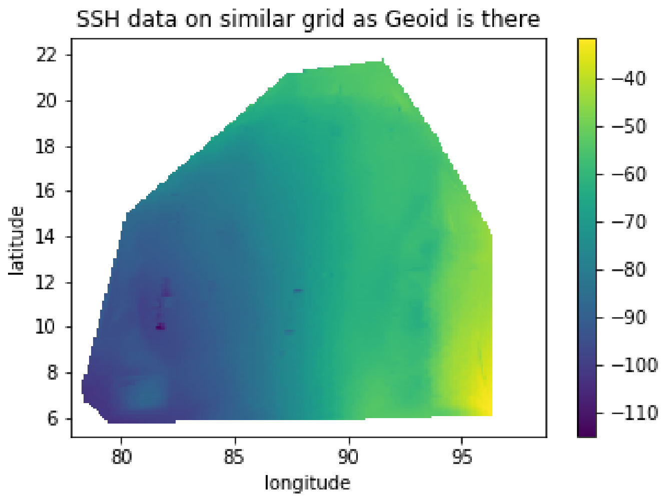

Fig. 8: Sea Surface Height data (Interpolated).

Figure 9 shows the interpolated SSH data with the Geoid contours overlapping to visualize them simultaneously.

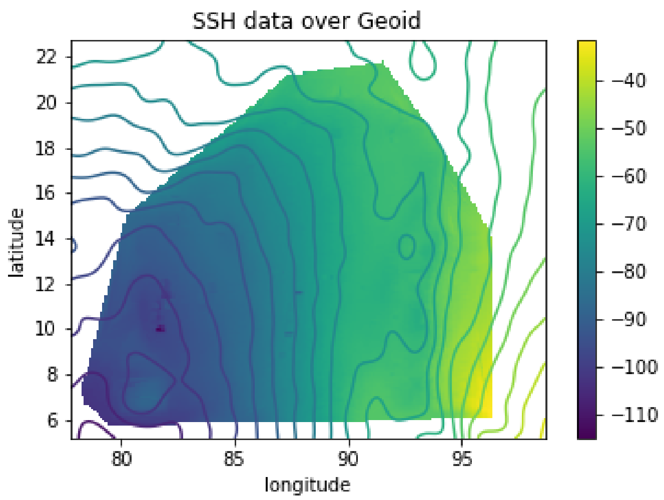

Fig. 9: Sea Surface Height overlap with Geoid data.

6.3 Mean Dynamic Topography

Now we are able to find mean dynamic topography by the formula $\overline{\eta} = \frac{\sum_t h(t)}{N} - N$. The obtained mdt is given in figure 10 shows the obtained raw MDT from simple computations. Still we can see some of the inconsistencies in the data with some outliers (Figrure 11). We need to filter this MDT to see the features clearly.

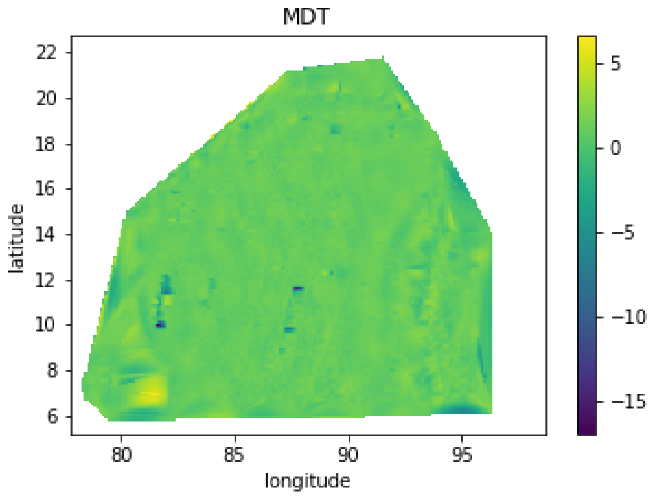

Fig. 10: Mean Dynamic Topography (MDT) $\overline{\eta}$

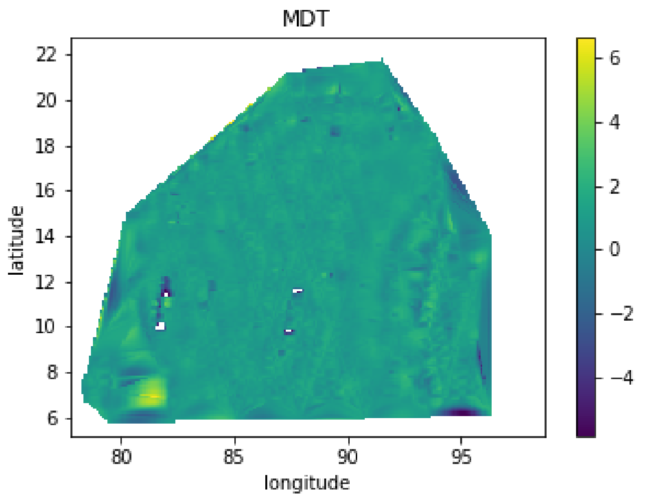

Fig. 11: Mean Dynamic Topography (MDT) $\overline{\eta}$ (Outlier Removal)

6.4 Filtering

There are many kind of filtering techniques that could be applied here but for the sake of simplicity we have used here Gaussian Blur as a filter with enough window size that the noise and outliers gets suppressed. Figure 12 shows the MDT after filtering.

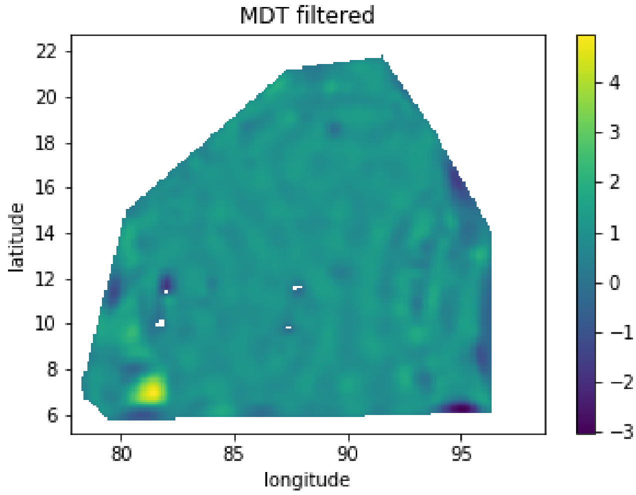

Fig. 12: Mean Dynamic Topography (MDT) $\overline{\eta}$ (Filtered)

6.5 Current component determination

Now we can determine the current components with the help of the following formulas:

$$
\begin{aligned}
&u = -\frac{\gamma}{fR}\frac{\partial \overline{\eta}}{\partial \phi} \\
&v = -\frac{\gamma}{fR\cos\phi}\frac{\partial \overline{\eta}}{\partial \lambda} \\
&\text{Where} \\
&f = 2\omega_e \sin\phi
\end{aligned}
\tag{4}
$$

Figure 13 shows the final current components obtained from the system.

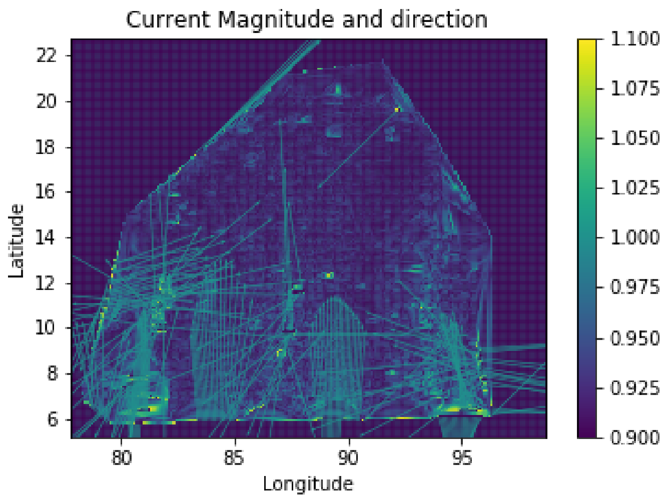

Fig. 13: Current Components with magnitude shown in the background.

6.6 Clustering of currents

As we have proposed the clustering of the currents, the idea seems to have some problem with the chaos in the land boundary. The results for the clustering is shown in the figure 14 shows the clustering of the currents in the given ROI. The results with the K-means are not so good the possible reasons are listed below:

1. The chaotic data at the boundaries.
2. Time lapse of the data is too small for any pattern.
3. The extent of data needs to be more.

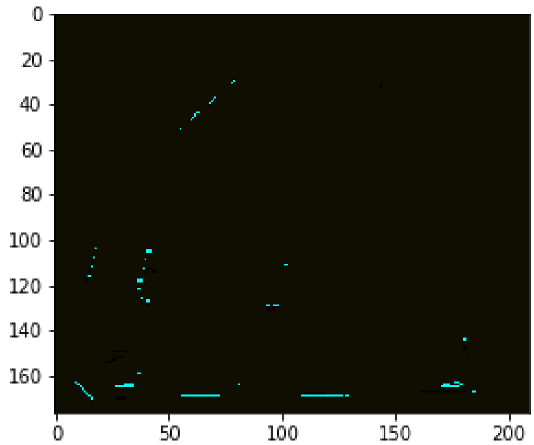

Fig. 14: Result of k-means clustering.

7 Conclusion

Concluding the project, we have shown the process and result of the ocean current decomposition, the results are interesting but there is some problem with the land and ocean boundary region, and there we get large boost in the readings. We need some way to remove them from our system in order to get more accurate visualization. The ocean currents analysis can give us better estimated of mineral flow and many more predictions so it's a need to get these more accurate.

References

Baltazar Andersen .Baltazar Andersen .2018. BaltazarAndersen2018Baltazar Andersen, O., Knudsen, P., Nielsen, K., Hughes, C., Williams, S., Bingham, R.Fenoglio-Marc, L. 2018. Dynamical Coastal Topography and tide gauge unification using altimetry and GOCE Dynamical Coastal Topography and tide gauge unification using altimetry and GOCE. Geophys. Res. Abstr.202018–14821.

Becker, Brockmann SchuhBecker .2014. Becker2014Becker, S., Brockmann, JM. Schuh, WD. 2014. Mean dynamic topography estimates purely based on GOCE gravity field models and altimetry Mean dynamic topography estimates purely based on GOCE gravity field models and altimetry. Geophys. Res. Lett.4162063–2069. 10.1002/2014GL059510

Bingham, Haines LeaBingham .2015. Bingham2015Bingham, RJ., Haines, K. Lea, D. 2015. A comparison of GOCE and drifter-based estimates of the North Atlantic steady-state surface circulation A comparison of GOCE and drifter-based estimates of the North Atlantic steady-state surface circulation (35) (PA). 10.1016/j.jag.2014.03.012

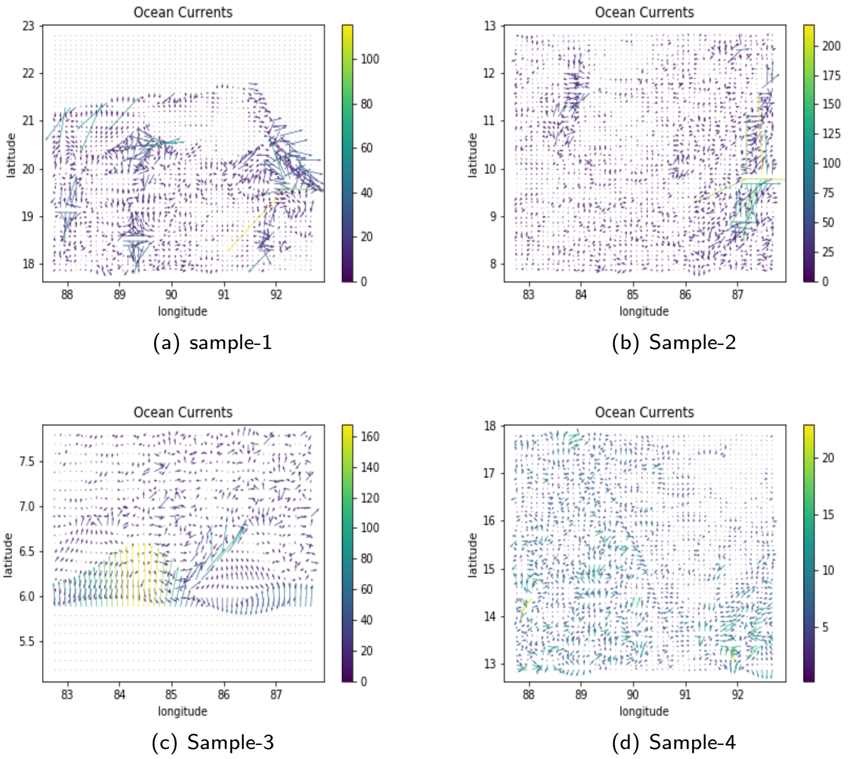

(a) sample-1

(b) Sample-2

(c) Sample-3

(d) Sample-4

Fig. 15: Sample Results

Bingham, Knudsen, Andersen Pail Bingham .2011. Bingham2011Bingham, RJ., Knudsen, P., Andersen, O. Pail, R. 2011. An initial estimate of the North Atlantic steady-state geostrophic circulation from GOCE An initial estimate of the North Atlantic steady-state geostrophic circulation from GOCE. Geophys. Res. Lett.3811–5. 10.1029/2010GL045633

ChristianChristian2012. Christian2012Christian, C. 2012. GOCE Data for Ocean Modelling Thesis submitted for the degree of philosophiae doctor GOCE Data for Ocean Modelling Thesis submitted for the degree of philosophiae doctor.

Haines .Haines .2011. Haines2011Haines, K., Johannessen, JA., Knudsen, P., Lea, D., Rio, MH., Bertino, L.Hernandez, F. 2011. An ocean modelling and assimilation guide to using GOCE geoid products An ocean modelling and assimilation guide to using GOCE geoid products. Ocean Sci.71151–164. 10.5194/os-7-151-2011

HercegHerceg. HerHerceg. . 5.1.1 Basic Principle – Radar Altimetry Tutorial and Toolbox. 5.1.1 Basic Principle – Radar Altimetry Tutorial and Toolbox. [2021-04-29]`http://www.altimetry.info/radar-altimetry-tutorial/how-altimetry-works/basic-principle/`

Janjić .Janjić .2012. Janjic2012Janjić, T., Schröter, J., Savcenko, R., Bosch, W., Albertella, A., Rummel, R. Klatt, O. 2012. Impact of combining GRACE and GOCE gravity data on ocean circulation estimates Impact of combining GRACE and GOCE gravity data on ocean circulation estimates. Ocean Sci.8165–79. 10.5194/os-8-65-2012

Knudsen, Bingham, Andersen Rio Knudsen .2011. Knudsen2011Knudsen, P., Bingham, R., Andersen, O. Rio, MH. 2011. A global mean dynamic topography and ocean circulation estimation using a preliminary GOCE gravity model A global mean dynamic topography and ocean circulation estimation using a preliminary GOCE gravity model. J. Geod.8511861–879. 10.1007/s00190-011-0485-8

Pail .Pail .2010. Pail2010Pail, R., Goiginger, H., Schuh, WD., Hck, E., Brockmann, JM., Fecher, T.Rieser, D. 2010. Combined satellite gravity field model GOCO01S derived from GOCE and GRACE Combined satellite gravity field model GOCO01S derived from GOCE and GRACE. Geophys. Res. Lett.37205015. 10.1029/2010GL044906

Rio, Mulet Picot Rio .2014. Rio2014Rio, MH., Mulet, S. Picot, N. 2014. Beyond GOCE for the ocean circulation estimate: Synergetic use of altimetry, gravimetry, and in situ data provides new insight into geostrophic and Ekman currents Beyond GOCE for the ocean circulation estimate: Synergetic use of altimetry, gravimetry, and in situ data provides new insight into geostrophic and Ekman currents. Geophys. Res. Lett.41248918–8925. 10.1002/2014GL061773

van der Meijde, Pail, Bingham Floberghagen van der Meijde .2015. VanderMeijde2015van der Meijde, M., Pail, R., Bingham, R. Floberghagen, R. 2015. GOCE data, models, and applications: A review GOCE data, models, and applications: A review. Int. J. Appl. Earth Obs. Geoinf.35PA4–15. `http://dx.doi.org/10.1016/j.jag.2013.10.001` 10.1016/j.jag.2013.10.001

Vigo, Sempere, Chao Trottini Vigo .2018. Vigo2018Vigo, MI., Sempere, MD., Chao, BF. Trottini, M. 2018. Mediterranean Surface Geostrophic Circulation from Satellite Gravity and Altimetry Observations Mediterranean Surface Geostrophic Circulation from Satellite Gravity and Altimetry Observations. Pure Appl. Geophys.175113989–4005. 10.1007/s00024-018-1911-0